LAWRENCE
LIVERMORE
NATIONAL
LABORATORY

LLNL-CONF-666703

Near Field Intensity Trends of Main Laser Alignment Images in the National Ignition Facility (NIF)

R. R. Leach, I. Beltsar, S. Burkhart, R. Lowe-Webb, V. Miller Kamm, T. Salmon, K. Wilhelmsen

January 29, 2015

SPIE Photonics West 2015
San Francisco, CA, United States
February 7, 2015 through February 12, 2015

Near Field Intensity Trends of Main Laser Alignment Images in the National Ignition Facility (NIF)

Richard R. Leach Jr., Ilona Beltsar, Scott Burkhart, Roger Lowe-Webb, Victoria Miller Kamm, Thad Salmon, Karl Wilhelmsen

Lawrence Livermore National Laboratory, 7000 East Avenue, Livermore, CA 94550

ABSTRACT

The National Ignition Facility (NIF) utilizes 192 high-energy laser beams focused with enough power and precision on a hydrogen-filled spherical, cryogenic target to potentially initiate a fusion reaction. NIF has been operational for six years and during that time, thousands of successful laser firings or shots have been executed. Critical instrument measurements and camera images are carefully recorded for each shot. The result is a massive and complex database or 'big data' archive that can be used to investigate the state of the laser system at any point in its history or to locate and track trends in the laser operation over time. In this study, the optical light throughput for more than 1600 NIF shots for each of the 192 main laser beams and 48 quads was measured over a three year period from January 2009 to October 2012. The purpose was to verify that the variation in the transmission of light through the optics over time performed within design expectations during this time period. Differences between average or integrated intensity from images recorded by the input sensor package (ISP) and by the output sensor package (OSP) in the NIF beam-line were examined. A metric is described for quantifying changes in the integrated intensity measurements and was used to view potential trends. Results are presented for the NIF input and output sensor package trends and changes over the three year time-frame.

Keywords: intensity ratio, big data archive, trend analysis, light transmission, beam path, exposure time

1. INTRODUCTION

The National Ignition Facility at the Lawrence Livermore National Laboratory has been operational since 2009 for the study of high-energy density and fusion science. One of three main goals in NIF is to study new regimes in astrophysics and basic science. The second main goal is to ensure the United States stockpile of nuclear weapons is and will remain reliable, safe, and secure. The third main goal for NIF is that of achieving ignition, which is to produce a net energy gain for the first time in a laboratory setting [1] [2] [3] which could lead to an abundant safe and carbon-free supply of electricity [4]. NIF consists of a 1.8 MJ ultraviolet laser system containing 192 beams and is capable of delivering up to 500 trillion watts of power onto a 2mm diameter target.

The NIF building is approximately 150m×90m and seven stories tall. It comprises 11 sections; two laser bays, four power conditioning bays, two beam switchyards, a target bay, a diagnostic building, and a core controls and oscillator area. A schematic of the building layout is shown in Figure 1.0. Each beam line follows a nominal path of 510 meters and contains 110 major optical components in addition to 600 alignment beams and 1400 alignment references. The principal opto-mechanical hardware includes approximately 825 charge coupled device (CCD) cameras, 9500 motors, 160 sensor packages, 215 calorimeters, 192 wave-front sensors and deformable mirrors, and 250 photodiodes [5]. In addition, control of supporting electronics for driving the hardware and precise and timely capture of diagnostic data are required.

Periodic monitoring of this complex system is an on-going effort at the NIF. One of the areas of interest is the light transmission as it travels through the main laser beam line optics. For example, in the main laser, each beam propagates through more than one hundred optics and reflects off of more than twenty optics between the Input Sensor Package (ISP) and Output Sensor Package (OSP). Monitoring the light transmission between the ISP and OSP gives the ability to detect degradation or unexpected behavior of laser transmission. In addition, light transmission measurements can potentially be used to adjust and improve laser performance models of the system [6].

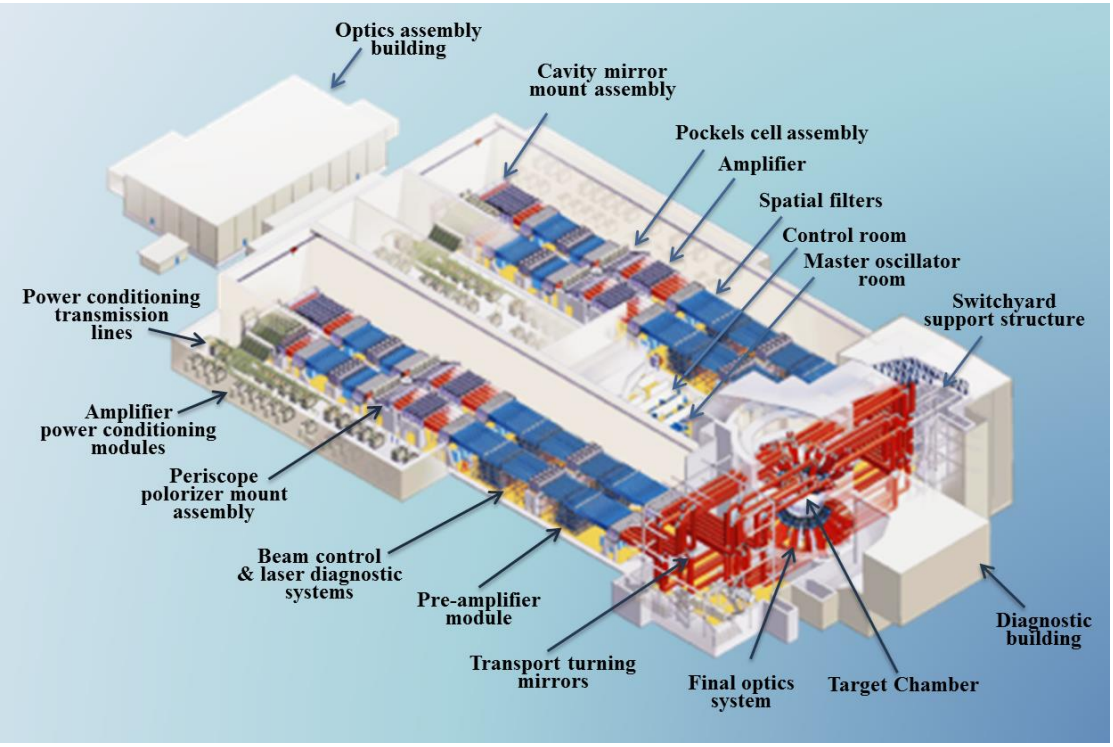

Figure 1.0 Schematic view of the National Ignition Facility highlighting some of the main elements of the laser system. For a sense of scale in this figure, the round target chamber on the right is 10 meters in diameter.

Although there are many theories for the causes of changes in the light transmission level, currently, they are only speculative. The hypothesized causes of transmission loss range from minor rotation errors of re-installed polarizers, fogging of reflective coatings, to solarization of the flash amplifier glass. As we improve our ability to measure transmission loss, we will be able to do further investigation of the causes of transmission loss. Sensor locations used for measuring main laser light transmission in this study are described in the next section.

2. NIF BEAM PATHS AND SENSOR SELECTION

A diagram of one of the 192 NIF beam paths is shown in Figure 2.0. The ISP is located at the beginning of the laser chain and at the output of the preamplifier module (PAM). The input sensor contains the diagnostic functions to measure the energy, temporal and spatial waveforms. A 1053nm, continuous wave (CW) alignment pilot laser beam is injected into the NIF beam path at the ISP after the pre-amplifier module where it is co-aligned with the NIF pulsed-beam via near field and far field reference fiducials at the respective relay planes. From this point, the beam-path of the alignment beam and NIF pulsed beam are nearly identical through the main laser to the output of the Transport Spatial Filter (TSF) vessel. A CCD camera system is used to capture both near field and far field alignment images, toggled by an insertable lens. The same camera is used to capture a near field image of the pulsed beam at shot time. Near the output of the ISP, the beam is split evenly four ways using a series of three, half-wave plates and three polarizers resulting in a single ISP beam that services four, or a 'Quad' set of main laser beams. Each beam is injected into the main laser via the TSF. The beam passes through the power amplifier once before entering the main amplifier cavity. The beam traverses the main amplifier four times before being ejected. A half-wave plate in the form of a Plasma Electrode Pockels Cell (PEPC) in pass two rotates the polarization of the NIF pulsed beam so that it passes through the polarizer and remains trapped in the main amplifier. The beam polarization is rotated ninety degrees again on pass three, allowing the beam to be reflected by the polarizer out of the main amplifier on pass four. The beam passes out of the main amplifier and through the power amplifier a second time and a tiny sample (nominally less than 0.5%) is reflected from the diagnostic beam-splitter just after collimation by the TSF output lens and sent to the OSP. The alignment beam, on the other hand, is

trapped in the main amplifier by insertable half-wave plates in the Cavity Spatial Filter (CSF) alignment tower in passes two and three instead of firing the PEPC. Further, the alignment beam is sampled by an insertable beam-splitter cube near the focus of the TSF and sent to the OSP.

A Quad of NIF beams is serviced by two OSP's. Each of the ninety-six OSPs are located below one of the twenty-four TSF towers and is optically coupled to the laser via a series of relay optics which include fixed and variable attenuators. Since the alignment beams are sampled near prime focus of the TSF and the pulsed beam is sampled by the diagnostic beam-splitter, separate alignment and diagnostic optical paths are provided coupling each to the same OSP. The OSP provides diagnostics that characterize the full beam line performance for a pair of beams including a CCD camera used to measure the near-field intensity distribution, a Hartmann camera used to measure wavefront, and a time resolved power sensor to record the temporal pulse shapes of the fully amplified beam. At shot time, the near field images of paired beams are imaged side-by-side by the CCD camera insuring every beam is imaged for every shot. Alignment images acquired during the alignment process leading up to a shot are also recorded and archived.

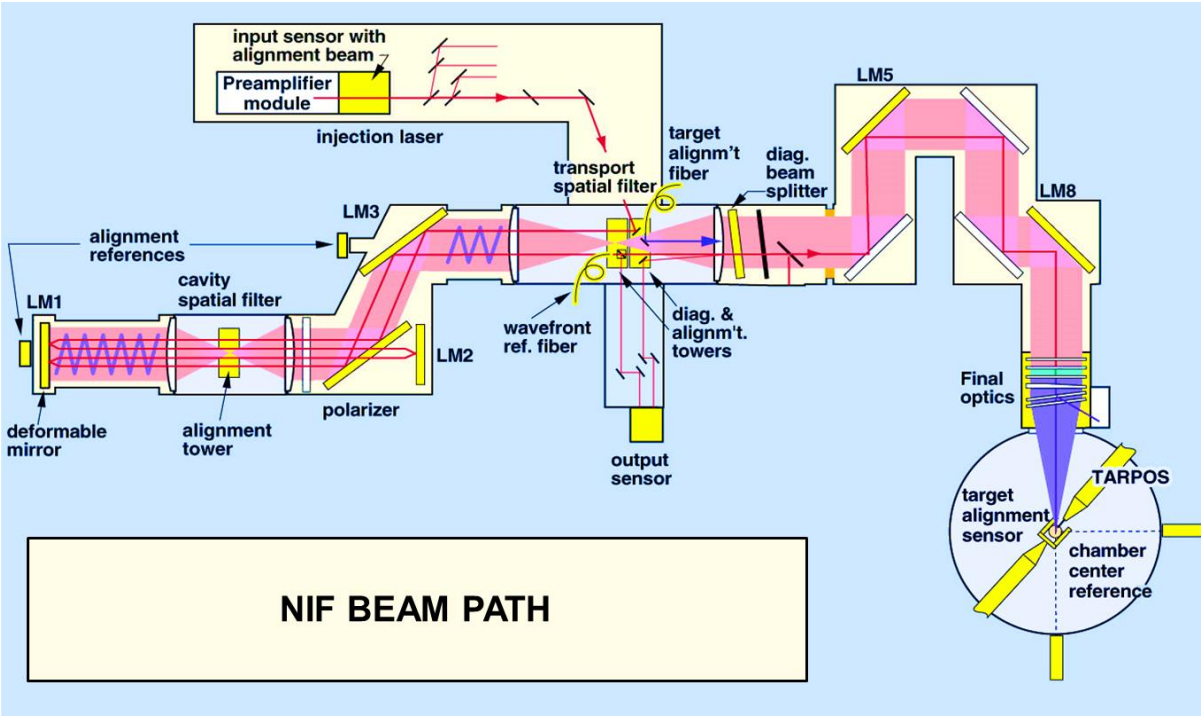

Figure 2.0 Diagram of one of the 192 NIF beam paths. Input sensor images (ISP CCD camera) were compared to output sensor (OSP CCD camera) images to measure light intensity changes over a period of three years. Components used for automated alignment and wave-front control are highlighted in yellow.

The ISP and OSP bracket the main laser and both are used to capture near-field alignment images. Subsequently, these images can be used to measure optical throughput. In this study, archived near-field alignment images acquired from both the ISP and the OSP cameras were analyzed to characterize the optical throughput of the main lasers. Specifically, the average intensities of the ISP image and the corresponding four OSP images were compared.

3. NIF ARCHIVED DATA

3.1 NIF Big Data

Over the years, NIF has archived a staggering amount of data including code, images, reports, parameters, and many other database records. As NIF grows and requirements change, database parameters give NIF the ability to adapt to those changes. In addition, NIF has moved to becoming an operational facility where detecting hardware degradation or improving adjustment efficiency has become a high priority. Using NIF big data to this end will continue to grow in importance as seen in the increased development of support and maintenance and commissioning (MCT) tools.

For this study, a handful of database parameters were required to verify that the change in light intensity through the main laser optics over time is performing within design expectations. Retrieval of archived main laser alignment images for all of NIF 192 beams for every laser firing was required. To accomplish this task manually would take many months or years; however NIF image downloader software and script tools were readily available and used to retrieve the hundreds of thousands of archived images.

In addition, millions of specified database parameters were needed for image exposure compensation. The NIF database team utilized NIF database query tools, and the needed parameters were accessed quickly and paired with their associated images for each time of any given shot. Leveraging NIF tools and capabilities condensed what would have been a two year study into a two month study. Figure 3.1 shows a snipped of the output of a typical database query done in this study.

SHOT_ID	ISP_LOCATION	ISP_REQUEST_ID	ISP_GAIN	ISP_TRANSMISSION_RATE	ISP_EXPOSURE_TIME	ISP_LOOP_NAME	SHOT_ID	OSP_LOCATION1	OSP_REQUEST_ID1	OSP_GAIN1	OSP_TRANSMISSION_RATE1	OSP_EXPOSURE_TIME1	OSP_LOOP_NAME1
N090109-001-999	Q12B	123149199003600	1	0.052591	0.15	AA_ISP_CL_ALIGNMENT	N090109-001-999	B125	123149231888400	1	0.001292	0.1	aa_isp_lm3_tsf_p4
N090109-001-999	Q12B	123149340077900	1	0.052591	0.15	AA_ISP_CL_ALIGNMENT	N090109-001-999	B125	123149231888400	1	0.001292	0.1	aa_isp_lm3_tsf_p4
N090109-001-999	Q12B	123149398724400	1	0.052591	0.15	AA_ISP_CL_ALIGNMENT	N090109-001-999	B125	123149231888400	1	0.001292	0.1	aa_isp_lm3_tsf_p4

Figure 3.1 Database parameters are critical tools that allow NIF to adapt to changes and to enable NIF the behavior of the system to be studied. Snippet of the output of a typical query for this study is shown with naming, beam and quad number, and parameters such as ISP camera gain set point.

The 48 quads in NIF are identified numerically by their location. The 192 beams in NIF are identified by a unique 3 digit code associated with one of the quads (4 beams per quad). For example Q11T denotes quad 11 and splits into four beam that propagate into the upper hemisphere of the target chamber. B111, B112, B113, and B114 are the four beams associated with Q11T. In the same manner Q11B splits into B115, B116, B117, and B118 and propagate into the lower hemisphere of the target chamber.

3.2 Pruning NIF data

Data with missing images or parameters was excluded from this study. Shot alignments that resulted in less than a complete set of five archived beams per quad were removed. There were also cases where off-normal images were found; e.g. blank or saturated images, which were excluded as well. Archived database parameter naming convention changes over the years made association between images and database parameters unreliable at times and resulted in some shots being removed. Fortunately, these events occurred rarely over the time period of this study and more than 90% of the data from all beam lines was retrieved and processed successfully.

4. CONSISTENT IMAGE PROCESSING

Measuring an estimate of the illumination for ISP and OSP beams from the NIF camera images requires a series of image processing steps to produce accurate and consistent mean intensity measurements over the large set of images taken over many years. To accomplish this, all images were processed in the same manner for each beam using like algorithms to minimize bias in the resulting intensity measurements. Figure 4.0 illustrates typical near field ISP and OSP images. Dark spots and dark squares are used during laser alignment [7].

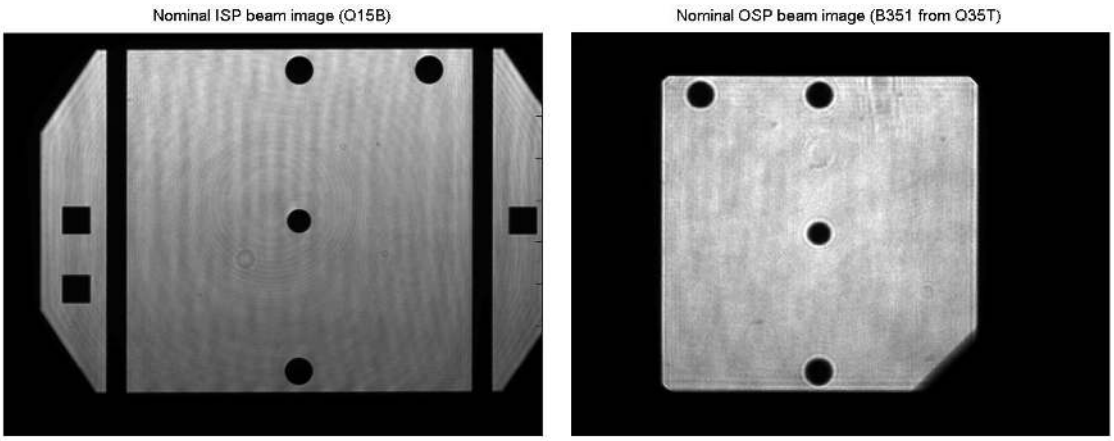

Figure 4.0 Example of typical main laser beam alignment image: ISP beam 351 in quad Q35 top (left). Dark spots are alignment features and are not present during system shots. Some beam corners are intentionally blocked for laser performance reasons. The OSP beam from quad Q15 bottom is shown on right. Alignment 'wings' to the left and right of the ISP beam are excluded from beam measurements.

4.1 Noise floor estimates

OSP and ISP camera sensors provide digitized 12 bit images. A histogram of intensity or exposure values from the camera image pixels is created. The lower intensity bins in the histogram compromise the image background. The beam can be seen in the higher intensity bins as a hump in the histogram. The noise floor was identified using a threshold parameter, nominally identified at ten percent of the peak of the lower intensity bins. This boundary occurs shortly after the sharp drop in the background noise histogram bins rolls off and flattens out as seen in figure 4.1.

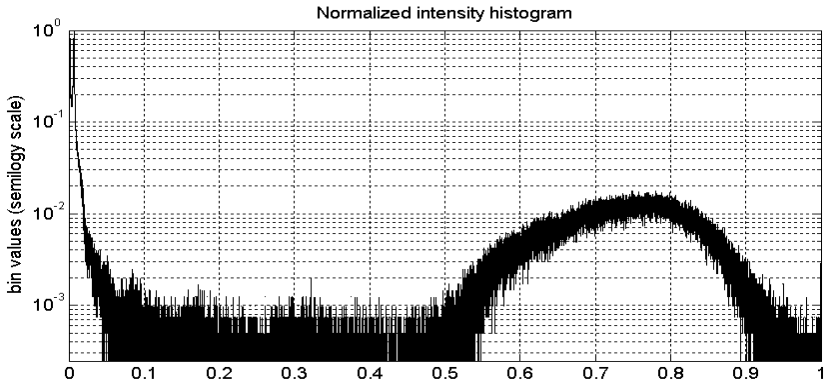

Figure 4.1 Normalized intensity histogram (from image in figure 4.0 left). The y axis is plotted in semi-log scale for clarity. The beam can be seen from about 0.5 to 0.9 while the noise floor threshold is approximately 0.1.

4.2 Beam top estimation

The top of the beam in the image should ideally appear flat, or with uniform intensity within the image. However, the beam consists of a dominant plane wave accompanied by smaller amplitude plane waves which appear as small intensity amplitude variations on what would otherwise have uniform intensity. A mean intensity value was calculated and used as the beam top as follows. Selected pixel values within the image were set to zero to exclude them in the measurement of the top of the beam. This included the noise floor pixels as well as the top 3% of the remaining image intensities to compensate for occasional glints or other stray light artifacts (typically reflected from the target) that may occur. A simultaneous left to right and top to bottom maximum projection lines from the image is seen as in the side and bottom plots in figure 4.2. The two plots were concatenated and used to calculate the average intensity of the signal, excluding zero values. The resulting average is used as the beam top location also shown in figure 4.3. The dark spots and blocked corners that appear in the images are excluded in the measurement using this measurement method.

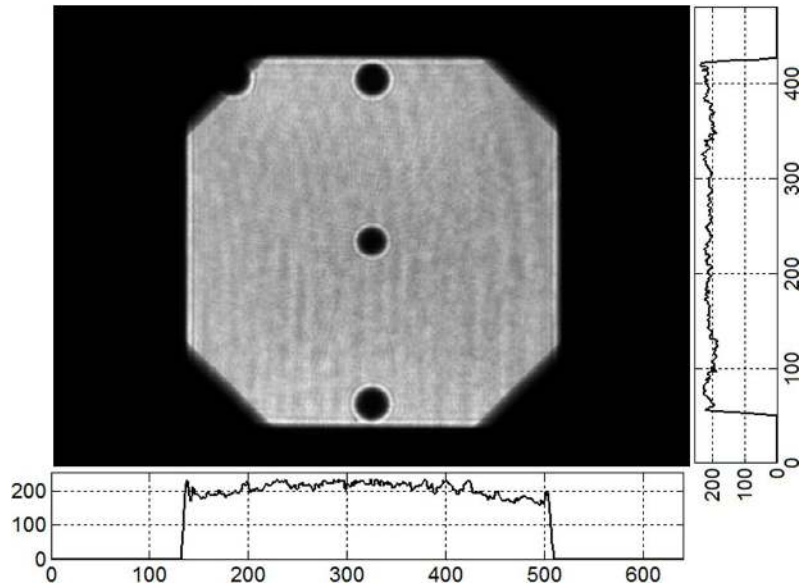

Figure 4.2 Maximum intensities per column (bottom) and per row (right) plots are shown for this example OSP image. Plot y axes indicate 8-bit intensity counts and x axis are the respective pixel column and row locations.

4.3 Beam footprint level selection

From the noise floor and the beam top measurements, the beam footprint at any intermediate level can be determined. Setting the level too low however, may introduce bias from noise floor fluctuations. Setting it too high can cause interference variations at the top of the beam. Based on the theoretical responses of coherent and incoherent systems to a step-function object, [8] the 25% beam level was used as a measure of the beam intensity for each ISP and OSP beam image to provide consistent measurements over time. The beam 25% level can be seen in Figure 4.3 as the lower superimposed dotted line.

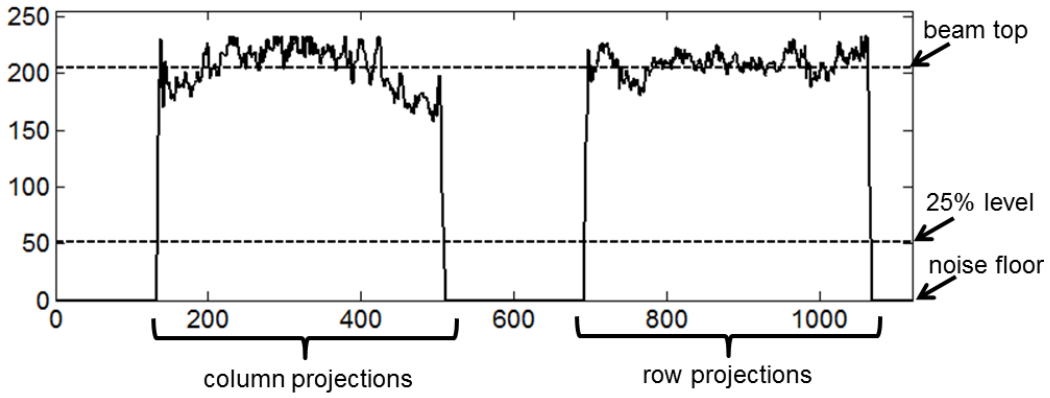

Figure 4.3 Maximum intensity per column and per row (right) are shown concatenated in this example. The noise floor is at zero. The beam top is the mean of the non-zero values in the signal and identifies the top of the beam.

4.4 Mean intensity estimates

The average intensity for each beam image was calculated using the set of pixels that are at or above the 25% beam level as described in the previous section and shown in equation (1). This results in a beam footprint that excludes the noise floor in addition to any beam pixels below the 25% beam level. It also excludes the dark spots and blocked corners that appear in the images. Figure 4.4 shows the edge or outline of the beam footprint at the 25% level superimposed on the associated OSP image.

$$N = \#\text{ pixels} \quad \text{at or above 25\% level}$$
$$I_{\mu} = \frac{1}{N}\sum_{i=1}^{N} x_i \quad \text{mean intensity} \tag{1}$$

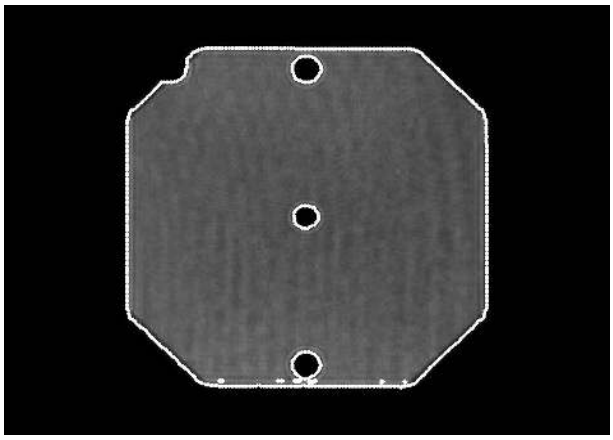

Figure 4.4 OSP image with 25% beam level outline superimposed in white. Pixel intensity values at or above this level are averaged to calculate the mean intensity for each ISP or OSP image.

4.5 Measuring image mean intensity and reviewing imagery over time

Image intensity for each set of ISP and OSP alignment images was measured for each NIF shot from January 2009 through October 2012. Figure 4.5 depicts one of the 48 NIF ISP quad images and its four associated OSP images. For each quad, a video was created using the five associated images from each shot as a single video frame. The video can be played in less than two minutes and shows over 1000 days of NIF shots in sequence. The videos were reviewed as an image integrity check to verify the history of the 48 ISP quads and 192 OSP beams for any time period and determine if there were any significant or unexpected changes, excluding systematic changes. Some examples of known systematic changes are the addition of corner blockers (figure 4.0) or change-outs of laser optics. From these images, a metric of image using the ratio of compensated mean or integrated intensities was calculated. The following section describes this metric.

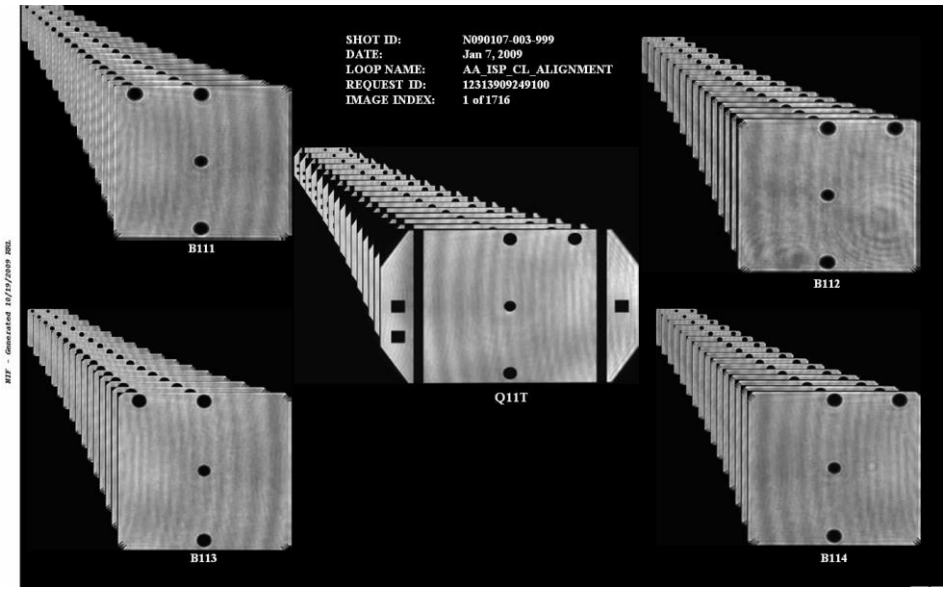

Figure 4.5 NIF quad Q11T top (center) ISP image and its four associated OSP (outer) images. This is one of 48 ISP quad and 192 OSP images used in this study. The mean intensity at the 25% beam level was measured over a three year period for all beam and quad images.

5. OPTICAL LIGHT INTENSITY METRIC

This section describes a metric that was developed as a measure of the ratio of integrated intensities of the ISP and OSP images for each laser after a shot. For each shot alignment, several parameters are set during the shot which are shot-specific. Due to differences in these settings, the ISP and OSP intensities at the 25% level cannot be compared directly. Mean intensity values must first be compensated with archived shot database parameters to avoid introducing systematic bias due to differing attenuator or camera settings.

5.1 Shot Database parameters

Many parameters are recorded during each NIF laser alignment performed prior to each shot. Three of these parameters were used in developing the metric used in this study. The first are the ISP and OSP attenuator transmission settings which were stored as attenuator set points. The second is the camera exposure integration times which are stored as camera set points for both the ISP and OSP cameras. The third is the ISP and OSP camera A-D gain settings for each archived image. All three parameters consisted of camera and attenuator set points constant values which were recorded during each respective laser alignment and recovered from a NIF database archive as shown in equation (2).

$$\begin{aligned} T &= \text{transmission rate} \\ E &= \text{exposure time} \\ G &= \text{gain} \end{aligned} \tag{2}$$

5.2 Light integrated intensity ratio metric

The mean intensity measurements determined by the image processing described in the previous section are next compensated using the three parameters (*TEG*). For the ISP measurements, the image intensity for each quad is divided by the product of its transmission rate and the exposure time and the gain as seen in equation (3).

Compensated ISP intensity (1 quad)

$$I_{ISP} = \frac{I_{\mu}}{TEG} \tag{3}$$

Similarly, for the OSP measurements, the image intensity for each of the four respective beams is divided by the product of its transmission rate and the exposure time. The mean OSP intensity is the combination of the average of the 4 individual beams as seen in equation (4).

Compensated OSP intensity (4 beams)

$$I_{OSP} = \frac{1}{4}\left(\frac{I_{\mu 1}}{T_1 E_1 G_1} + \frac{I_{\mu 2}}{T_2 E_2 G_2} + \frac{I_{\mu 3}}{T_3 E_3 G_3} + \frac{I_{\mu 4}}{T_4 E_4 G_4} \right) \tag{4}$$

From (2) and (3), the light integrated intensity metric is then defined by the ratio of the two compenstated intensity estimates as follows.

$$M = \frac{I_{OSP}}{I_{ISP}} \tag{5}$$

The result is the integrated intensity ratio metric (M) which was calculated from all NIF alignment data from 2009 to 2012 and used to track trends in optical throughput from ISP to OSP.

5.3 Parameter Variation (TEG)

The TEG parameter set points values may or may not change over time. For example, the camera gain was set to one for the entire time period of this study for both the ISP and OSP camera set points. However, attenuator transmission set points or camera exposure set points were changed occasionally due to changes in the alignment laser for both the ISP and OSP cameras. Figure 5.3 shows an example of the changes in TEG or Q11T and B111. Changes do not occur often, sometimes months or years apart. Also, changes in TEG parameters tend to pre-date laser replacements and may be useful as an indicator for laser maintenance.

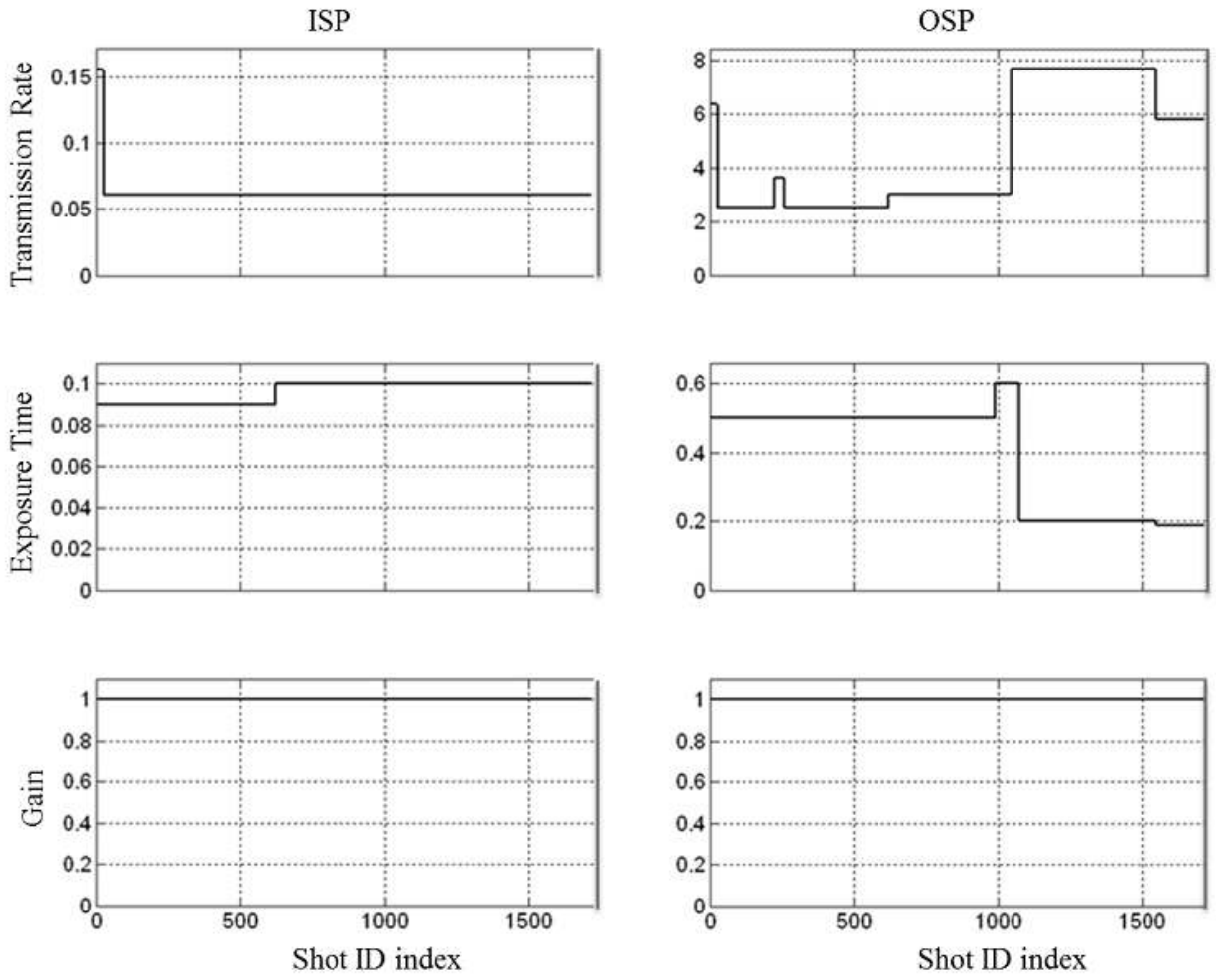

Figure 5.3 TEG parameters from the time period 2009 through 2012 for ISP quad Q11T (left column) and OSP beam B111 (right column). The camera gain for both the ISP and OSP camera did not change (Gain=1) for the entire time (bottom row). Changes do not occur often, sometimes months or years apart as seen in the ISP transmission rate that was adjusted once over the time period.

6. RESULTS AND DISCUSSION

Results are presented for two quads, Q11T and Q16T using data from the ISP and four associated OSP images. Table 6.0 shows the average value and the standard deviation of the integrated intensity ratio metric M from January 2009 to October 2012 for each quad. The standard deviation of M is under 2.5% for both quads and is within design expectations. Plots of the intensity ratios are shown in the next two sections.

Table 6.0 Integrated intensity ratio metric (M) trends for two of the 48 NIF quads from January 2009 to October 2012.

Integrated intensity ratio metric (M)	**Q11T**	**Q16T**
mean μ	41.1	40.1
Standard Deviation σ	0.99	0.66
Time period	2009-2012	2009-2012
Number of shots	1717	1667

6.1 NIF Quad 11 top or Q11T results

Results are shown in Figure 6.1 for Quad 11 top (Q11T) for all NIF shots from 2009 thru 2012. The OSP integrated intensity I_{OSP} appears as the top signal in the upper plot. The ISP integrated intensity I_{ISP} appears as the middle signal in the upper plot and ratio M appears as the bottom signal in the top plot. For Q11T, M appears to diminish over time, yet the output light follows the same trend and the metric M remains mostly unperturbed. The discontinuities in the two upper signals are coincident with scheduled alignment laser replacements. The lower plot is a closer look at the integrated intensity ratio metric M with mean removed. There appears to be a slight downward trending in the ratio over the three years of the data for this quad.

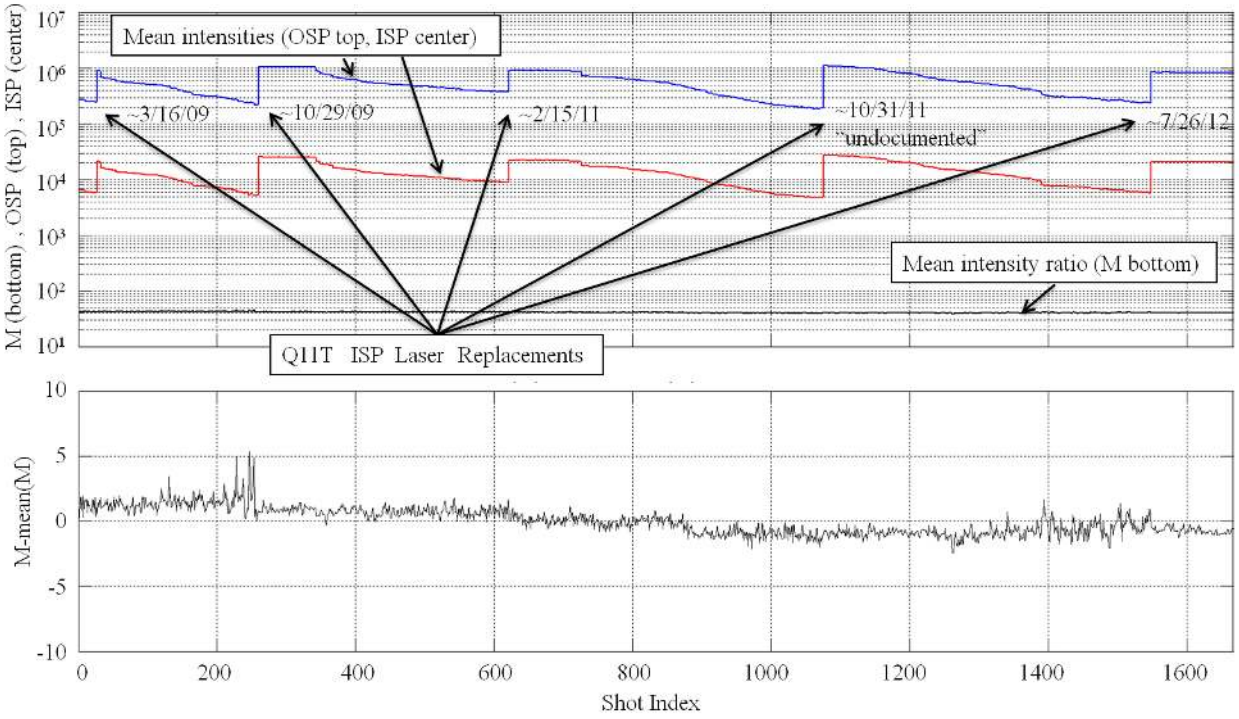

Figure 6.1 Results are shown for Quad 11 top (Q11T) for all NIF shots from 2009 thru 2012. The OSP integrated intensity I_{OSP} appears as the top signal in the upper plot. The ISP integrated intensity I_{ISP} appears as the middle signal in the upper plot and ratio M appears as the bottom signal in the top plot. The discontinuities in the two upper signals are coincident with scheduled laser replacements. The lower plot is a closer look at the integrated intensity ratio metric M with mean removed.

6.2 NIF Quad 16 top of Q16T results

The Results are shown for Quad 16 top (Q16T) for all NIF shots from 2009 thru 2012. Again, the OSP integrated intensity I_{OSP} appears as the top signal in the upper plot, The ISP integrated intensity I_{ISP} appears as the middle signal in the upper plot and ratio M appears as the bottom signal in the top plot. There were no known alignment laser replacements during the time of this study as reflected by the comparative smooth signals as compared to Q11T. The lower plot is a closer look at the integrated intensity ratio metric M with mean removed. There appears to be no downward trending in the ratio over the three years of the data for this quad.

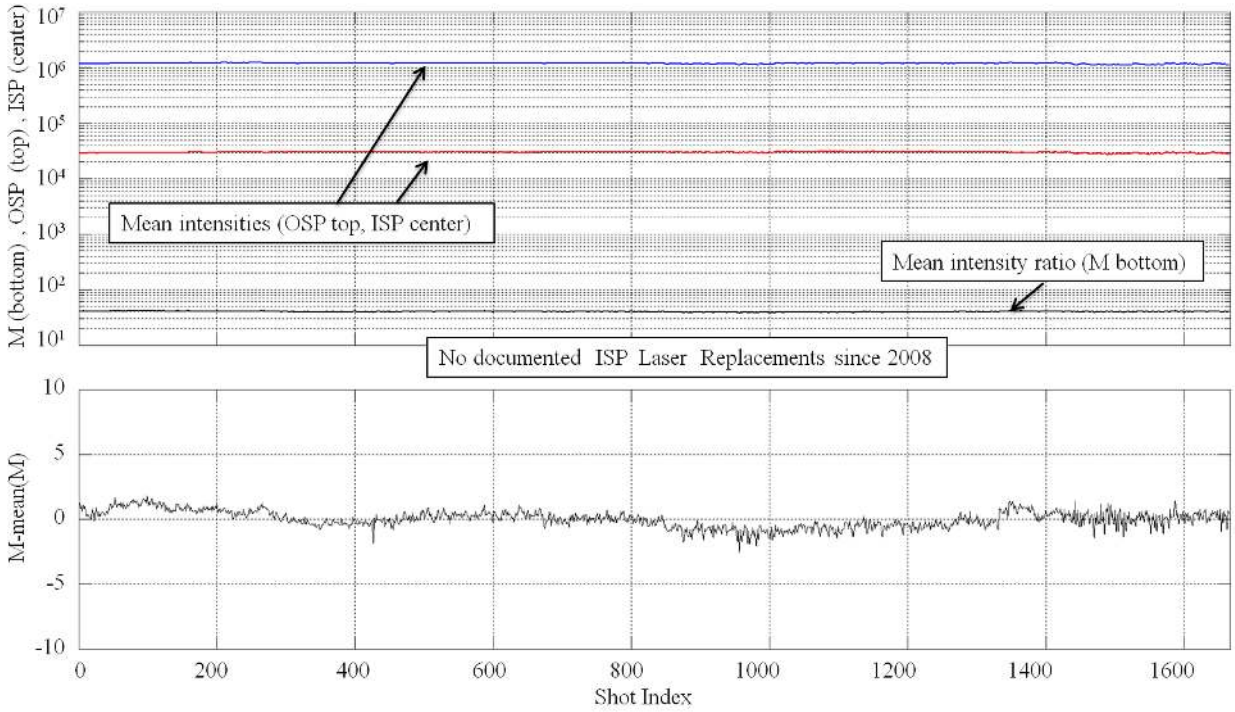

Figure 6.2 Results are shown for Quad 16 top (Q16T) for all NIF shots from 2009 thru 2012. The OSP integrated intensity I_{OSP} appears as the top signal in the upper plot, The ISP integrated intensity I_{ISP} appears as the middle signal in the upper plot and ratio M appears as the bottom signal in the top plot. There were no known laser replacements during the time of this study as reflected by the comparative smooth signals as compared to Q11T. The lower plot is a closer look at the integrated intensity ratio metric M with mean removed.

7. CONCLUSIONS AND FUTURE WORK

The main conclusion from this study is that the metric of the OSP/ISP integrated intensity ratio *M* is a useful indicator of optical throughput from ISP to OSP. The signal shows very little change over three years with a variance under 2.5%. There is some indication the metric is susceptible to alignment laser replacements which is potentially due to attenuator calibration issues. There is also some indication of an increase in noise prior to alignment laser replacements in Q11T. Although no major changes are occurring, errors could be further reduced by reconciling the measurements with machine history half-wave plate positions. In future work, the remaining quads will be plotted and analyzed. In addition it would be useful to investigate the effects of CCD attenuator calibrations on the intensity ratio metric.

8. SUMARY

The NIF facility has archived a massive and complex database or 'big data' archive which was used in this study to track light integrated intensity trends in the NIF ISP and OSP laser sensor packages over a three year operating period from January 2009 to October 2012. More than 1600 shots were mined for their archived alignment images and associated parameters in order to verify that the change in light transmission through the ISP and OSP optics performed within design expectations. Differences between average intensity from images recorded at the input sensor package and at the output sensor package in the NIF beam-lines were examined. A metric was developed for quantifying the ratio *M* of the input and output sensor average integrated intensity and the resulting trends. Results were presented that illustrate the change in M over the three year timeframe was within design expectations. The potential benefit of using the integrated intensity ratio for trend analysis of optical throughput in laser systems was also illustrated.

ACKNOWLEDGEMENTS

This work performed under the auspices of the U.S. Department of Energy by Lawrence Livermore National Laboratory under Contract DE-AC52-07NA27344. The authors would like to thank the database team and their extremely useful database query tools that provided access to parameters without which this study could not have been done. We would also like to thank Philip Adams for his image downloader software and script tools used to retrieve thousands of archived images.

REFERENCES

[1] [E. I. Moses, The National Ignition Facility and the National Ignition Campaign", Vol. 38 No. 4, IEEE Transactions on Plasma Science, Apr, 2010

[2] E. I Moses, "Ignition on the National Ignition Facility: a path towards internal fusion energy", **49**, Nuclear Fusion, IOP Publishing and International Atomic Energy Agency, Sep, 2009

[3] C. A. Haynam, P. J. Wegner, G. M. Heestand, E. Moses, R. A. Sacks, M. W. Bowers, S. N. Dixit, G. V. Erbert, M. A. Henesian, M. R. Hermann, K. S. Jancaitis, K. Knittel, T. Kohut, K. R. Manes, C. D. Marshall, N. C. Mehta, J. Menapace, J. R. Murray, M. C. Nostrand, C. D. Orth, R. Patterson, R. Saunders, M. J. Shaw, M. Spaeth, and S. B. Sutton, "The National Ignition Facility: Status and Performance of the World's Largest Laser System for the High Energy Density and Inertial Confinement Fusion", in *Conference on Lasers and Electro- Optics/Quantum Electronics and Laser Science Conference and Photonic Applications Systems Technologies*, OSA Technical Digest (CD) (Optical Society of America, 2008), paper CFQ1.

[4] Karl Wilhelmsen, G. Brunton, S. Burkhart, D. McGuigan, V. Miller Kamm, R. Leach Jr., R. Lowe-Webb, R. Wilson, Status of the automatic alignment system for the National Ignition Facility, Fusion Engineering and Design, *Proceedings of the 8th IAEA Technical Meeting on Control, Data Acquisition, and Remote Participation for Fusion Research*, **87**, 1989-1993, December 2012

[5] R. D. Boyd, E. S. Bliss, S. J. Boege, R. D. Demaret, M. Feldman, A. J. Gates, F. R. Holdener, J. Hollis, C. F. Knopp, T. J. McCarville, V. J. Miller-Kamm, W. E. Rivera, J. T. Salmon, J. R. Severyn, C. E. Thompson, D. Y. Wang, R. A. Zacharias, "Alignment and diagnostics on the National Ignition Facility Laser System", *Proc. SPIE* 3782, Optical Manufacturing and Testing III, 496, November 11, 1999.

[6] Michal Shaw, Wade Williams, Ronald House, Chris Haynam, Laser Performance Operations Model (LPOM), Optical Engineering, *Special Section on Fusion Laser Engineering*, **43**, 2885-2895 December 2004

[7] S. C. Burkhart, E. Bliss, P. Di Nicola, D. Kalantar, R. Lowe-Webb, T. McCarville, D. Nelson, T. Salmon, T. Schindler, J. Villanueva, and K. Wilhelmsen," National Ignition Facility System Alignment", Applied Optics, Vol. 50, Issue 8, pp. 1136-1157 (2011)

[8] Joseph W. Goodman, [Introduction to Fourier Optics], McGraw Hill Companies, New York et al.,158-160 (1988)